



## Ultrasound well below the intensity threshold of cavitation can promote efficient uptake of small drug model molecules in fibroblast cells

Fabio Domenici, Claudia Giliberti, Angelico Bedini, Raffaele Palomba, Fabio Luongo, Simona Sennato, Cristina Olmati, Deleana Pozzi, Stefania Morrone, Agostina Congiu Castellano & Federico Bordi

To cite this article: Fabio Domenici, Claudia Giliberti, Angelico Bedini, Raffaele Palomba, Fabio Luongo, Simona Sennato, Cristina Olmati, Deleana Pozzi, Stefania Morrone, Agostina Congiu Castellano & Federico Bordi (2013) Ultrasound well below the intensity threshold of cavitation can promote efficient uptake of small drug model molecules in fibroblast cells, *Drug Delivery*, 20:7, 285-295, DOI: [10.3109/10717544.2013.836620](https://doi.org/10.3109/10717544.2013.836620)

To link to this article: <https://doi.org/10.3109/10717544.2013.836620>



Published online: 18 Sep 2013.



Submit your article to this journal [↗](#)



Article views: 472



Citing articles: 12 View citing articles [↗](#)

## ORIGINAL ARTICLE

## Ultrasound well below the intensity threshold of cavitation can promote efficient uptake of small drug model molecules in fibroblast cells

Fabio Domenici<sup>1</sup>, Claudia Giliberti<sup>2</sup>, Angelico Bedini<sup>2</sup>, Raffaele Palomba<sup>2</sup>, Fabio Luongo<sup>1</sup>, Simona Sennato<sup>1,3</sup>, Cristina Olmati<sup>4</sup>, Deleana Pozzi<sup>5</sup>, Stefania Morrone<sup>6</sup>, Agostina Congiu Castellano<sup>1</sup>, and Federico Bordi<sup>1,3</sup><sup>1</sup>Physics Department, Sapienza University, Rome, Italy, <sup>2</sup>INAIL, Italian Workers' Compensation Authority, Rome, Italy, <sup>3</sup>Physics Department, CNR-IPCF UOS Roma, Sapienza University, Rome, Italy, <sup>4</sup>Tuscia University, Germplasm Bank, Viterbo, Italy, <sup>5</sup>Department of Molecular Medicine, Sapienza University, Rome, Italy, and <sup>6</sup>Department of Experimental Medicine and Pathology, Sapienza University, Rome, Italy

## Abstract

Ultrasound (US) induced enhancement of plasma membrane permeability is a hugely promising tool for delivering exogenous vectors at the specific biological site in a safe and efficient way. In this respect, here we report effects of membrane permeability alteration on fibroblast-like cells undergoing very low-intensity of US. The change in permeability was pointed out in terms of high uptake efficiency of the fluoroprobe calcein, thus resembling internalization of small cell-impermeable model drugs, as measured by fluorescence microscopy and flow cytometry. Fluorescence evidences moreover suggests that the higher the time of exposure, the larger will be the size of molecules can be internalized. The uptake events were related to the cell viability and also with structural changes occurring at membrane level as revealed by infrared spectroscopy and preliminary membrane fluidity and atomic force microscopy (AFM) investigation. Thus, the question of whether the uptake of cell-impermeable molecules is consistent with the presence of disruptions on the cell membrane (sonopore formation) has been addressed. In this framework, our findings may constitute experimental evidence in support of sub-cavitation sonoporation models recently proposed, and they may also provide some hints towards the actual working condition of medical US dealing with the optimum risk to benefit therapeutic ratio.

## Keywords

Fluorescence microscopy, NIH-3T3, sonoporation, ultrasonic delivery, ultrasound

## History

Received 29 May 2013  
Accepted 13 August 2013  
Published online 17 September 2013

## Introduction

Over the last few years an ever growing biophysical interest has seen and are being addressed on the ability of ultrasound (US) (waves above 20 kHz frequencies) to transfer mechanical energy into cells allowing for transient enhancement of membrane permeability (Mitragotri, 2005; Newman & Bettinger, 2007; Mason, 2011). The phenomenon, known as reparable sonoporation (Mitragotri, 2005; Newman & Bettinger, 2007; Mason, 2011) is a very effective modality for drug delivery and gene therapy because energy that is non invasively transmitted through the skin can be focused deeply into the human body in a specific location and employed to release drugs at that site in a safe and efficient way (Newman & Bettinger, 2007; Mason, 2011).

It is thought that in a fluid medium undergoing an US field the energy transfer is primarily mediated by the cavitation activity of gas bubbles, that is known as the steady pulsations

(stable cavitation) or rapid collapse (inertial cavitation) generated from submicron-sized gas pockets called cavitation nuclei. According to sonoporation studies (Schlicher et al., 2006; Newman & Bettinger, 2007), cavitation-promoted plasma membrane wounds, can allow the uptake of poorly membrane-permeable exogenous vectors in viable cells, although the lack of reversibility of the process results in cell death (Schlicher et al., 2006). Some applications may benefit from killing cells (Ward et al., 2000), however, drug delivery scenarios seek to maximize intracellular uptake while holding cell viability constant (Guzmán et al., 2002; Deng et al., 2004). Unfortunately, higher US dosage than necessary may increase the risk of having cavitation related side effects such as sonochemically and thermally induced denaturations, irreversible damages at lipid membrane, protein and DNA levels (Ward et al., 2000; Guzmán et al., 2002; Deng et al., 2004; Schlicher et al., 2006), thus threatening the human healthy.

In this respect, low-intensity non cavitation US exposures (spatial peak temporal average intensity,  $I_{ta} < 100 \text{ mW/cm}^2$ ) have been reported (Krasovitski et al., 2011) to induce bioeffects such as membrane deformation and permeability increasing without evidence of inertial or stable cavitation being present. In the attempt to figure out how also low intensity US can effect cell plasma membrane, a unifying

Address for correspondence: Fabio Domenici, Physics Department, Sapienza University, Rome, Italy. Tel: +39 0649913503. Fax: +39 0697893304. Email: [fabiodomenici@gmail.com](mailto:fabiodomenici@gmail.com)  
Claudia Giliberti, INAIL, Italian Workers' Compensation Authority, Rome, Italy. Tel: +39 0697893312. Fax: +39 0697893304. Email: [c.giliberti@inaail.it](mailto:c.giliberti@inaail.it)

mechanism has been recently proposed by computational and experimental evidences carried out at molecular *in vitro* and *in vivo* levels (Krasovitski et al., 2011). Dynamics response on hydrated model membrane ( $K_s = 30\text{--}120$  pN/nm) exposed to continuous US pressure regime of oscillations (0.1–1 MPa) at 1 MHz has been predicted to exhibit strong leaflets deformation and membrane detachment processes. The phenomenon has been figured out in terms of a “positive” (compression) pressure, where it pushes water molecules closer to each other, and “negative” (rarefaction) values, when the water molecules are pulled away from each other against cohesion forces. The large membrane areal strain allows for rising the leaflet tension, substantially to maximum levels of about 10 and 16 pN/nm. These values appear to be larger than the tension capable of causing polyunsaturated lipid bilayers to rupture (3–10 pN/nm). Notably, they are also close to 38 pN/nm, being the theoretical tension required to generate hydrophilic pores in a bilayer membrane (Lee et al., 2008; Krasovitski et al., 2011).

That novel awareness may open the actual possibility to drive biological properties of cellular membranes as a safe, efficient and smart way for transferring DNA, drugs or other molecules in target viable cells. Despite several evidences of the beneficial use of US to improve the uptake of different drugs, to date significant variations in the efficacy of US-induced permeabilization of biological membranes have been reported (Guzmán et al., 2001a; O’Brien, 2007). In particular, the quantitative dependence of small compound uptake into viable cells on US exposure parameters in sub cavitation conditions, to positively influence the therapeutic effect (Guzmán et al., 2001a; O’Brien, 2007; Grimaldi et al., 2011), is not well documented and is the subject of this study.

Our work has been focused to a medical US device (Grimaldi et al., 2011) providing 1 MHz frequency at different low  $I_{ta}$  and exposure times of therapeutic relevance. As *in vitro* cell model the well known NIH murine fibroblast-like culture (NIH-3T3) has been considered. As a small cell-impermeable model drug we choice to use the fluoroprobe calcein (radius = 0.6 nm) (Kodama et al., 2000), a negatively charged molecule that cannot cross intact eukaryotic cell membranes. Hence it is extensively used in order to assess membrane injury-promoted uptakes, where internalization or leakage of calcein can instead occur through the plasma membrane, in spite of the electrostatic repulsion, only due to the occurrence of an additional passive diffusion gradient. The dynamic of calcein uptake in US cavitation regime in the low frequency range (20–100 kHz) is well known and analyzed in several papers (Kodama et al., 2000; Guzmán et al., 2001b; Schlicher et al., 2006), also using 3T3 mouse cell suspension (Sundaram et al., 2003). They have also enlightened (Schlicher et al., 2006) that intracellular uptake scaled proportionally with extracellular calcein concentration between 1 and 1000  $\mu\text{M}$ , which is consistent with concentration-dependent diffusion, or convection, through membrane disruptions. Also fluorescein isothiocyanate (FITC)-dextrans at different sizes have been also employed to analyze if beside the enhanced ATP-dependent uptake previously reported for higher US intensity (Kodama et al., 2000; Meijering et al. 2009) also in this case a sonoporation mediated uptake may take place.

In this framework, firstly flow cytometry and fluorescent microscopy have been employed to evaluate intracellular uptake of fluoroprobes. Then, the here reported effects of membrane permeability alteration has been used to better understand vibrational Fourier transform infrared spectroscopy (FTIR) analysis of the lipid structure on 3T3 cells as well as preliminary evidences of US-related mechanical stress on cell plasma membrane. Thus, the question of whether the presence of disruptions on the cell membrane (pore formation) is consistent with the uptake of cell-impermeable molecules has been addressed.

## Materials and methods

### Cell culture

The experiments were carried out using murine fibroblasts NIH-3T3. The cells were cultured as a monolayer in a humidified atmosphere with 95% air and 5%  $\text{CO}_2$  at 37 °C in Dulbecco’s modified Eagle’s medium (DMEM, Sigma-Aldrich, St. Louis, MO) with 10% fetal bovine serum, 1% penicillin and 1% glutamine/streptomycin, in well plates (Falcon® Easy Grip™ tissue culture dish, 35 × 10 mm) at concentrations varying between  $7 \times 10^5$  cells/ml and  $9 \times 10^5$  cells/ml. Three milliliters of cell suspension were used in each experiment.

Sample viability was determined by propidium iodide (PI) test which was better than 95% for each trial.

### Ultrasound setup

For the US exposures, we used a medical device consisting of two submersible piezoceramic circular transducer (6 cm diameter) tuned at 1 MHz (maximum nominal intensity =  $2.5 \text{ W/cm}^2$ ). Such system can work in the range from 10 to 100% of the maximum power, in continuous and pulsed mode. In the pulsed mode, the duty cycle can be selected: in high mode, the signal is delivered for 750 ms, followed by a pause of 250 ms. The ultrasonic transducer was placed at the bottom of a tank 30 × 30 × 30 cm filled with degassed water. A Petri dish hermetically lidded ( $9.6 \text{ cm}^2$ ), containing the cell culture in adhesion, was positioned at the water surface and inserted to half of its thickness in the bathroom, in line with the transducer, according to the scheme in Figure 1. The temperature of the bath was kept constant at about 25 °C.

The characterization of the acoustic field produced by the US source was performed within the Petri dishes by using a needle hydrophone Precision Acoustics of 1 mm diameter (S.N. 1470) with sensitivity 1670.4 mV/MPa ( $\pm 14\%$ ) at 1 MHz. The biological samples were sonicated at ultrasonic source-dish surface distance (SSD) of 5 cm (at which the US field was evaluated as stable and reproducible) for exposure times of 5, 15, 30, 45 and 60 min.

In this work, the intensity of the acoustic field is provided in terms of  $I_{ta}$  that represents the maximum spatial intensity measured when the pulse is on, mediated for the period of pulse repetition and it is commonly used to correlate bioeffects induced by low intensity pulsed US (Krasovitski et al., 2011).

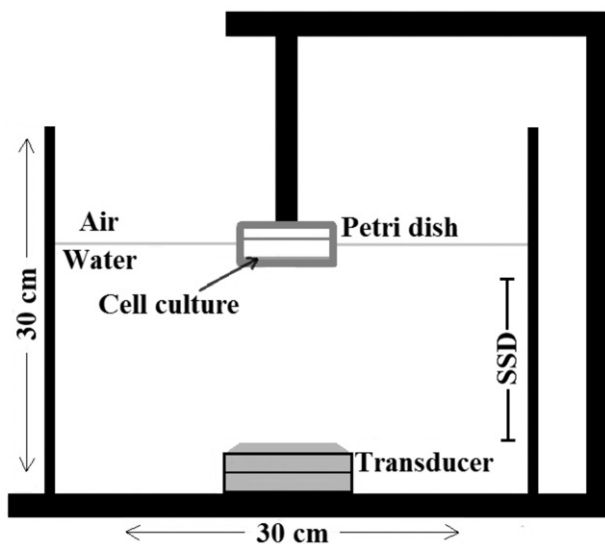


Figure 1. Schematic sketch of the experimental setup for ultrasound exposures.

Table 1. The sub-cavitation US  $I_{ta}$  values investigated.

$I_{ta}$ 1 MHz (mW/cm <sup>2</sup> )
11.8
15.2
19.3

The exposure  $I_{ta}$  values on 3T3 cells were set significantly below the recommended threshold of cavitation regime of 100 mW/cm<sup>2</sup> and are reported in Table 1.

### Optical measurements

For fluorescence measurements an inverted optical microscope Leica DM IL (Obj 10 $\times$ , 20 $\times$ , 40 $\times$ ) equipped with Hg vapor lamp and filters DAPI/FITC/TRITC, was used. The morphological changes in cellular samples exposed to US were captured by a digital camera Olympus for the acquisition of frames. The cells were incubated in Petri dishes until confluence and the sonications were performed in Dulbecco's phosphate-buffered saline (PBS): just before US application, a solution of a fluorescent dye, calcein (Molecular Probes, Eugene, OR, wavelengths of the maximum absorption and emission peak respective at 494 and 514 nm) was added to the wells to attain a final concentration of 10  $\mu$ M (Guzmán et al., 2002). Calcein is a green fluorescent molecule that cannot cross intact cell membranes. At the end of the sonication, in agreement with the literature (Schlicher et al., 2006), a recovery of 10 min was scheduled, and then washes with PBS buffer to eliminate calcein not internalized were provided. Non viable cells were identified by uptake of PI (PI, 20  $\mu$ l, molecular weight (MW) = 668.4 Da and wavelength of maximum absorption peak and emission respective 535 and 617 nm), a probe that can be internalized through damaged plasma membrane and it is intercalated into hydrophobic space of cellular DNA, emitting fluorescence. It is added just before analysis.

For fluorescence measurements using fluoroprobes FITC-dextrans were performed exposing 3T3 cell to US at fixed  $I_{ta}$  11.8 mW/cm<sup>2</sup> and varying the time of exposure at 15, 30 and 60 min in presence of 10  $\mu$ M of FITC labeled dextrans at MW of 10, 40 and 70 kDa, respectively, and waiting more than 10 min upon US field is stopped to allow the recovery of equilibrium membrane condition. Upon the Petri dish was carefully rinsed in PBS buffer several different areas were observed using a 10 $\times$  objective (100 $\times$  total magnification) of the inverted, phase contrast fluorescence microscope Leica DMIL, endowed with a 100 W mercury vapour lamp, FITC filter set, and coupled with high resolution and sensitivity CCD photocams (Jenoptik and Zeiss AxioCam ICc3) driven by Zen 2011 software (Göttingen, Germany).

### Flow cytometry measurements

Flow cytometry was performed using fluorescence activated cell sorting (FACS) cytometer FACSCalibur (BD Biosciences, San Jose, CA) equipped with two excitation lasers (argon  $\lambda = 488$  nm and visible red diode laser 635 nm); 10 000 events were recorded for each sample. Sample preparation and treatment steps were performed according to the fluorescent microscopy procedure and the use of PI (10  $\mu$ l) to identify non viable cells. At the end of each sonication, the samples were detached from Petri dishes, centrifuged (1800 rpm) in PBS buffer, collected in tubes suitable for cytometry and labeled with PI, added just before analysis.

Flow cytometry was used to detect the number of cells stained with calcein probe, indicating cell permeabilization, and cells stained with PI, indicating necrotic cell. Cells emitting fluorescent intensity higher than those of sham control were classified as permeabilized. Results were expressed in percentage of positive cells (% gated), using CellQuest software (Becton Dickinson, Franklin Lakes, NJ). Of practical significance is the ratio of cells in which permeability increase is induced by US to those that are killed by the same US exposure, defined as "therapeutic ratio" TR for sonoporation.

### FTIR spectroscopy measurements

The spectroscopic measurements were performed with Jasco spectrophotometer FT-IR 410 in transmission mode; for each intensity and exposure time, cells were grown to confluence on a window of CaF<sub>2</sub> (diameter 2.5 cm) previously treated with a polylysine substrate in order to promote cell attachment. Cells on CaF<sub>2</sub> window was sonicated, washed in PBS and dried in a desiccator; then spectra were collected. For each trial, a control spectrum contemporary with sonicated samples spectra were acquired at 4 cm<sup>-1</sup> resolution and 64 interferograms. The IR spectra of the treated and untreated cells were acquired in the range of 3000–2800 cm<sup>-1</sup>, identifying the region of membrane lipids. All spectra were corrected for baseline, and processed using the software OPUS 5.0 (Bruker Optik, Billerica, MA). For each sample, the average spectrum of three experiments was analyzed.

All experiments were performed in triplicate. Results are reported and displayed as mean  $\pm$  standard deviation. Test of significance were performed using one-way analysis of variance (ANOVA  $p < 0.05$ ). The IR spectra were processed

Table 2. Efficiency (mean  $\pm$  standard deviation) of calcein uptake of 3T3 undergoing 1 MHz US on varying  $I_{ta}$  and time of exposures measured by FACS (% gated).

	$I_{ta} = 11.8 \text{ mW/cm}^2$	$I_{ta} = 15.2 \text{ mW/cm}^2$	$I_{ta} = 19.3 \text{ mW/cm}^2$
Control $2.6 \pm 1.1$			
$t = 30'$	$64.6 \pm 1.3$	$74.8 \pm 2.9$	$49.4 \pm 1.6$
$t = 45'$	$87.0 \pm 1.7$	$84.1 \pm 4.1$	$86.8 \pm 1.5$
$t = 60'$	$99.5 \pm 0.5$	$97.5 \pm 0.9$	$99.3 \pm 0.5$

by taking the second derivative of the second Savitzky–Golay algorithm with nine points smoothing.

## Results and discussion

### FACS and fluorescence microscopy evidences of sonoporation

The effects of alteration of membrane permeability induced by 1 MHz US, under the exposure conditions specified in ‘‘Materials and methods’’ section (see Table 1), have been investigated, with sensitive microscopic techniques as fluorescence microscopy and FACS by using the fluorescent probe calcein. The flow cytometry allows to quantify cells labeled with the fluorophore calcein. The results of exposure, expressed in percentage of positive cells (% gated) and reported in Table 2, show a high calcein uptake in the sonicated samples (84–99%) compared to the control (2%). Notably for sonication times above 45', an  $I_{ta}$  independent saturation effect for the internalization of the fluorophore occurs.

The corresponding cell treatments of 45', being characterized by high level calcein uptake, have also been investigated by fluorescence microscopy. The images shown in Figure 2(a) representative for  $I_{ta} = 11.8 \text{ mW/cm}^2$  reveal that exposures to US produce internalization of the fluorescent probe calcein in spite of a slight increase in cell death. Anyway according to the efficiency of uptake provided in Table 2 starting from 45' the effect of internalization has resulted almost independent to the  $I_{ta}$  here considered. As shown in Figure 2(b), it is also notably that calcein is uniformly distributed in the cytosol of cells, which is in accordance with literature reporting comparatively higher intensities of US treatments (Kodama et al., 2000). More interesting, even displaying of several different images it is rather sporadic to evidence both PI and calcein (Figure 2b, right side) colocalized within a single 3T3 cell. Thereby we can assert that the US-induced membrane permeability alteration allowing for internalization of calcein in 3T3 cell can be repaired and thereby the cell can keep calcein and viability as well.

It is also worth of noting that the present results, being pointed out operating at 1 MHz in subcavitating conditions (see ‘‘Introduction’’ section) using the probe calcein whose mechanism of cell internalization has been reported, exposing cells under US cavitation regimes, to be essentially due to concentration-dependent diffusion, or convection, through membrane disruptions (Schlicher et al., 2006) may be accounted for by the bilayer sonophore model (Krasovitski et al., 2011) in which the dynamic behaviour of lipid membrane undergoing US is depicted. Simulations based on this model have in fact shown that biological membranes

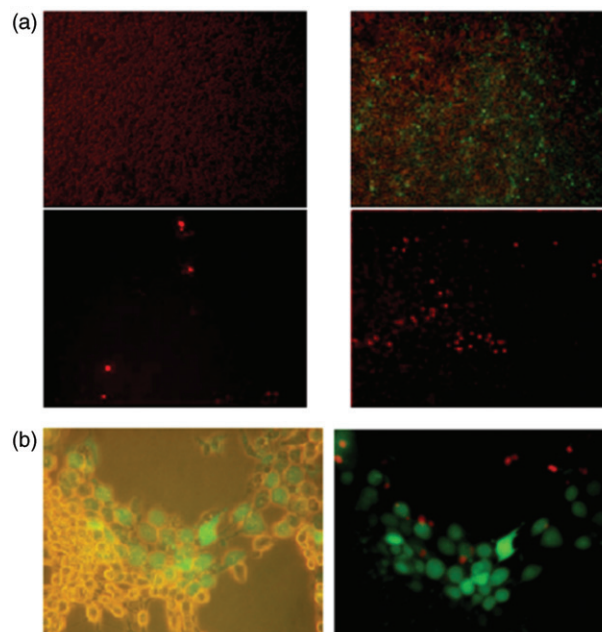


Figure 2. (a) Left side: FITC fluorescence together with low intensity transmitted phase contrast microscopy image of the sham control of 3T3 culture (up) and corresponding TRITC fluorescence of dead cells by PI assay (down); right side: representative fluorescence images of 3T3 culture treated with calcein together with US (1 MHz,  $I_{ta} = 11.8 \text{ mW/cm}^2$ , 45'), calcein diffused into viable cell in green light (up) and corresponding dead cell in red light (down). Images were acquired at 10 $\times$  of magnification. (b) Detail of 3T3 cell culture upon US treatment (1 MHz,  $I_{ta} = 11.8 \text{ mW/cm}^2$ , 45') in presence of calcein (left side): bright light and FITC fluorescence equipment was used simultaneously in order to clearly allocate fluorescent and non-fluorescent structures; the same culture treated with PI (right side): pass band FITC emission filter was used to simultaneously capture calcein and PI emission band. Images were acquired at 40 $\times$  of magnification.

exposed to 1 MHz can suffer a dynamic response capable of raising the elastic tension of the bilayer lipid membrane, close to the values required for the establishment of hydrophilic pores in the membrane (Lee et al., 2008; Krasovitski et al., 2011).

Notably as shown in Table 2 the uptake efficiency at a fixed intensity, for instance  $I_{ta} = 11.8 \text{ mW/cm}^2$ , increases by exposition time from 30 to 60 min. According to the sonoporation hypothesis (Krasovitski et al., 2011) this could mean that the higher the time of exposure the higher the probability to find cells with membrane injury large enough to make calcein able of enter the cell. On the contrary, as previously reported in literature (Lionetti et al., 2009), specific physical stimulus, such as US-mediated mechanical forces induced by US, may also alter endocytic pathways to promote targeted delivery of peptides, DNA and other biotherapeutic compounds across cell membranes. A peculiar characteristic of diffusion mediated by sonopores is that the membrane wound should not be formed instantaneously at its maximum size (Gelderblom et al., 2013). It is expected that upon the membrane wound is formed, US mediated energy transfer to the cytoplasm membrane, and in turn, increasing the time of exposure of US at a fixed intensity (Guzmán et al., 2001b), should reasonably provide the increment of the wound area to let the probe enter the cell (Guzmán et al., 2001b; Gelderblom et al., 2013). In other words, at variance of ATP-mediated endocytosis pathways (or other effects such

as activation of mechanosensitive channel proteins and increased membrane fluidity), increasing time of exposure should lead to gain the possibility to deliver higher MW molecules.

It is within this working hypothesis that here we show further fluorescence measurements we have undertaken in order to understand if the uptake here observed is probe size dependent. To this aim we expose 3T3 cell to US at fixed  $I_{ta}$  11.8 mW/cm<sup>2</sup> and varying the time of exposure at 15, 30 and 60 min in presence of 10 μM of FITC labeled dextrans at MW of 10, 40 and 70 kDa, respectively, and waiting more than 10 min upon US field is stopped to allow the recovery of equilibrium membrane condition. After rinsing the Petri dish carefully in PBS buffer we analyze several different areas using a total magnification of 100× and the representative pictures are shown in Appendix. The results clearly indicate that upon 15 min of exposition significant number of cells can internalize 10 and 40 kDa as well, the latter resulted slightly elevated with respect to corresponding sham control; upon 30 min the density of cell which have internalized 10 and 40 kDa are further increased (and are quite similar) but without evidences of internalization for 70 kDa. Only upon 60 min of exposure significant internalization of 70 kDa occurs. Also in this case we note that almost the cells which have internalized dextran hold own viability.

In literature, it has been reported that US and microbubble-targeted delivery of macromolecules such as dextrans in endothelial cells is regulated by induction of active endocytosis pathways and pore formation as well (Kodama et al., 2000; Meijering et al., 2009). Using 1 MHz pulsed US with 0.22 MPa peak-negative pressure (about one order of magnitude higher of the values here employed) fluorescence microscopy showed homogeneous distribution of 4.4 and 70 kDa dextrans through the cytosol, and localization of 155 and 500 kDa dextrans in distinct vesicles after internalization. After ATP depletion, reduced uptake of 4.4 kDa dextran and no uptake of 500 kDa dextran was reported (Meijering et al., 2009). This means that also in this case the sonoporation contribution to the dextran uptake is undoubtedly size dependent. Moreover, since our results show a clear size dependence uptake, we suspect that in our case perhaps due to the lower intensity involved, in our US setup passive diffusion represents the important transport mechanism.

Similar to what happen for calcein fluoroprobe, upon US field was ceased the recovery of wild-type membrane permeability features of 3T3 cells was observed.

We would stress that the size-dependent uptake of dextrans herein reported deals strongly in favour of an efficient sonopore-mediated passive diffusion mechanism. On the other hand, the enhanced uptake of 70 kDa dextran could not be promoted by the increased size of the hypothesized sonopore on 3T3 plasma membrane but also through the activation of some ATP-mediated endocytosis. Indeed as shown in Appendix the images shows that beside homogeneous distribution of dextrans we observed within the most of 3T3 cells, localization of 70 kDa dextran after 60 min of exposition has been observed in some cell, so that that the inclusion of dextran molecules in distinct endocytic vesicles (Meijering et al., 2009) may be also inferred.

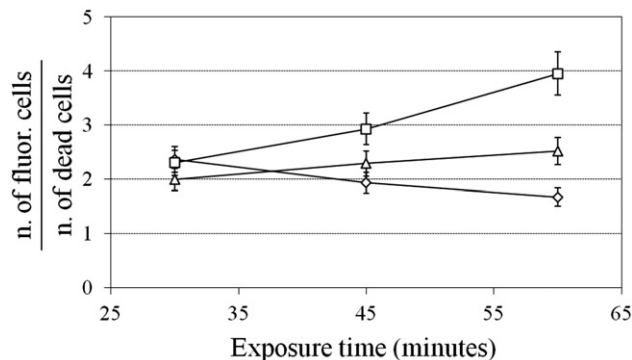


Figure 3. Ratio of fluorescent to dead cells (therapeutic ratio) as a function of the sonication time in the configurations investigated (see also ‘‘Ultrasound setup’’ section):  $I_{ta} = 11.8 \text{ mW/cm}^2$  ( $\Delta$ ),  $I_{ta} = 15.2 \text{ mW/cm}^2$  ( $\diamond$ ),  $I_{ta} = 19.3 \text{ mW/cm}^2$  ( $\square$ ).

On the basis of the information obtained in the present paper the contribution of additional concomitant effects to the observed enhanced uptake cannot be ruled out. However, a more comprehensive knowledge of which mechanisms of membrane transport are altered by very low intensity US intensity was not the aim of the present work.

PI viability test, applied to treated samples has been compared to the test applied to control sample: the results show that all sonicated samples have a viability lower than the control, with statistically significant negative correlation between the exposure time and the viability has been pointed out at  $I_{ta} = 11.8 \text{ mW/cm}^2$  ( $r = -0.9354$ ,  $p = 0.0061$ ).

The optimization of the uptake process provides a balance between the desired effect of the US exposure (uptake) and the destructive effect (cells death); for this purpose, a ‘‘therapeutic ratio’’ has been defined (TR, Figure 3) (Karshafian et al., 2009). The results show that the TR value depends on the exposure conditions; for the experimental configurations investigated, the maximum of the TR is obtained for  $I_{ta} = 19.3 \text{ mW/cm}^2$ ,  $t = 60'$ , in consideration of a high membrane permeability induced by exposure (99.27%) and reduced mortality of samples (25%), while the minimum is observed for the same time at  $I_{ta} = 11.8 \text{ mW/cm}^2$ .

#### FTIR analysis of lipid chains and preliminary related cell membrane structural information

We have studied the spectrum of the control sample in the wavenumber range from 3000 to 2800 cm<sup>-1</sup> (Figure 4a); the assignment (Mourant et al., 2003) of the main absorption peaks found in the IR spectra is reported in Table 3.

In order to detect structural changes in membrane lipid chains of 3T3 cells undergoing US, the  $R_i$  spectral parameters were defined. These indicators want to compare the area of the bands in Table 3 of the sonicated sample and area of the same bands of the control sample. Thereby, the  $i$  index becomes  $L_1$  and  $L_2$  ( $R_{Li}$ ).

The trends of the  $R_{L1}$  parameters versus exposure times for different  $I_{ta}$ , have been reported in Figure 4(b). The  $R_L$  parameter was considered varying significantly with increasing the time of exposure. Notably, at  $I_{ta} = 15.2 \text{ mW/cm}^2$  for the sonication time of 60' and at  $I_{ta} = 11.8 \text{ mW/cm}^2$  for

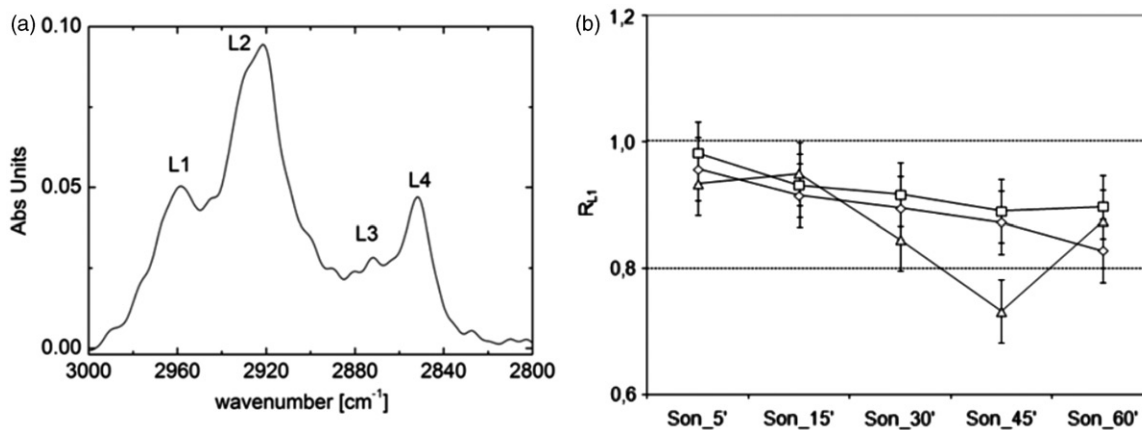


Figure 4. (a) The IR control spectrum of NIH-3T3 cells with the absorption bands. (b) Changes in the  $R_{L1}$  parameters versus sonication times relative to the  $L_1$  infrared band (see Table 3);  $I_{ta} = 11.8 \text{ mW/cm}^2$  ( $\triangle$ ),  $I_{ta} = 15.2 \text{ mW/cm}^2$  ( $\diamond$ ),  $I_{ta} = 19.3 \text{ mW/cm}^2$  ( $\square$ ).

Table 3. Peak labels and relative assignment of the main IR absorption bands of 3T3 cells falling among 3000–2800 cm<sup>-1</sup>.

Label	Peak (cm <sup>-1</sup> )	Assignment
$L_1$	2960	–CH <sub>3</sub> asymmetric stretching
$L_2$	2924	–CH <sub>2</sub> asymmetric stretching
$L_3$	2872	–CH <sub>3</sub> symmetric stretching
$L_4$	2852	–CH <sub>2</sub> symmetric stretching

$t = 45'$ ,  $R_{L1}$  highlights significant changes in the asymmetric structures of membrane phospholipids.

It is worth to be noted that since the FTIR spectra were acquired immediately upon treatments, a close relationship among the increasing alterations in both lipid membrane structure and uptake efficiency of calcein (reported in the previous section by FACS) may be inferred.

Mechanical stresses induced by US on plasma membrane are in fact closely connected to their physical features. In this connection, the FTIR analysis has led us to extensive further studies (currently under investigation), which are being focused on carrying out mechanical and phase membrane alterations also on a nanometric scale. More specifically, we have performed preliminary membrane fluidity tests using fluorescence Laurdan generalized polarization (GP) method (Parasassi et al., 1997) on NIH-3T3 cells exposed to US at  $I_{ta} \sim 10 \text{ mW/cm}^2$ . The measurements were performed immediately after the US was stopped. We found that starting to 15 min of exposition the membrane undergoes a significant loss of fluidity. In particular, GP percentage shifts from  $-8\%$  to about  $+10\%$  after 45 min of exposition. This should mean that intact membranes undergoing low intensity US stress cannot facilitate the diffusion of water as well as small hydrophilic molecules within the cytosol.

As it is known, the loss of membrane fluidity is consistent with an increased stiffness (in other words the elastic module) of membrane surface, and the effect is not surprisingly if we suppose that according to the literature (Lee et al., 2008; Krasovitski et al., 2011) an additional strength provided by US may occur. In the latter framework, the evaluation of local mechanical properties of the living cells at nanometric spatial resolution and force sensitivity (Kuznetsova et al., 2007) has

been pointed out on human keratinocyte HaCat cell line by atomic force microscopy (AFM) employing Harmonix modulus mapping of a DIMENSION ICON microscope equipped with a Nanoscope V Controller (Bruker AXS, Germany). Both treated and control cultures were fixed by glutaraldehyde cross linking (0.1%, for 30 min) before the US is stopped to attempt of fixing the membrane state undergoing the US insult. After careful rinsing with iso-osmolar solution the stiffness distribution has been obtained on several different single cells. Our preliminary results point out a redistribution of membrane stiffness, centred to  $\sim 0.950 \text{ GPa}$  for the control samples (which is the order of magnitude reasonably expected for Harmonix (Kuznetsova et al., 2007; Dokukin & Sokolov, 2012) on outer keratinocytes, fixed and measured in low RH condition) towards a ‘‘stiffer’’ corresponding structure, centred nearly  $2 \text{ GPa}$  for US exposure at  $I_{ta} \sim 10 \text{ mW/cm}^2$  for 45 min. Although keratinocytes exhibit different membrane structure and higher stiffness than that of fibroblasts, the result goes in the same direction of what observed by Laurdan GP analysis on 3T3 cells. Laurdan GP as well as AFM Harmonix data analysis we have herein hinted will be shown in more depth in a dedicated further coming work.

Taking also this aspects in mind the hypothesized affection in lipid structure exhibited in sonicated 3T3 as measured by FTIR spectroscopy seems to be consistent with some change in membrane lipid packages which may occur as a consequence of corresponding alteration of wild-type fluidity/elasticity features of 3T3. On this line, a FTIR-fluorescence combined approach may be useful in ease monitoring the structural and permeability behavior in plasma membrane cells such as threshold of US intensity at which the sonoporation occurs, maximum size of molecules which can entry and period for which the pores remains open.

## Conclusions

Changes in cell permeability and viability of murine fibroblasts *in vitro* induced by therapeutic US have been here evidenced under sub cavitation regimes, using flow cytometry and fluorescent microscopy, and have been related to the alteration of lipid structure composing the plasma membrane by FTIR spectroscopy.

Our results indicate that calcein is able to enter efficiently in fibroblast cells demonstrating the actual possibility of operating US mediated *in vitro* drug delivery at 1 MHz under very low intensity of exposure. Calcein uptake efficiency appears to be strongly increased by time of exposure, in spite of a slight lack of viability. Moreover, for 10–70 kDa FITC-dextran a size-dependent uptake related with time at a fixed intensity of exposure has also been enlightened. Corresponding changes in 3T3 membrane lipid structure has also been clearly evidenced. The findings may be consistent with previous reports suggesting the occurrence of subcavitation sonoporation although concomitant enhancement of other endocytosis effects cannot be here ruled out.

In order to provide the optimum in US exposure here examined for cell delivering of the small drug model molecule calcein into fibroblast cell model 3T3, the balance between the uptake and cells death has been analyzed pointing out the best therapeutic ratio for  $I_{ta} = 19.3 \text{ mW/cm}^2$  and 60'.

We are confident that our results may be helpful in shedding new light towards a more comprehensive knowledge of actual bioeffects which can be aroused at low intensity US in the direction of biomedical applications.

### Declaration of interest

The authors report no conflicts of interest. The authors alone are responsible for the content and writing of this article.

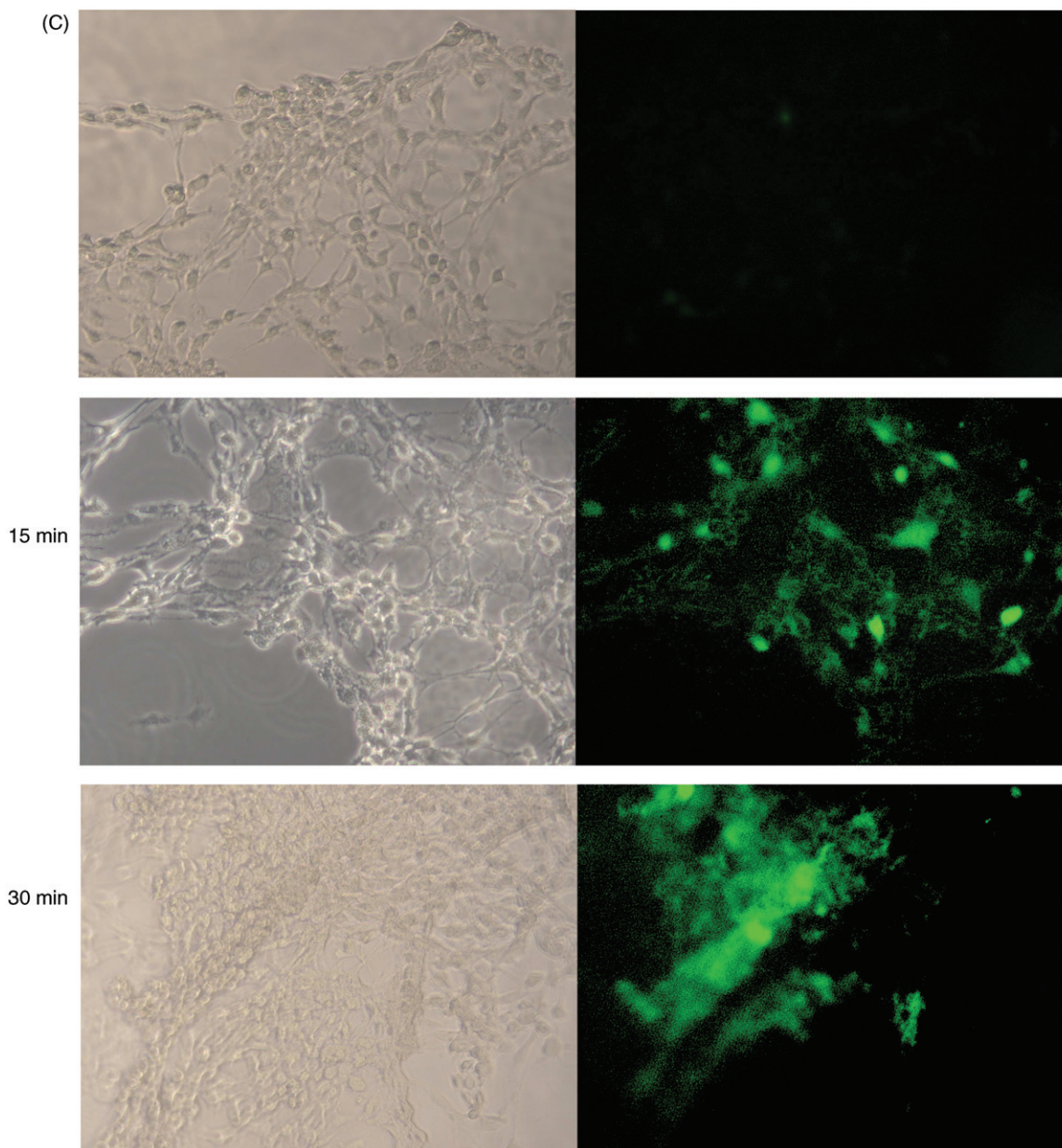
### References

- Deng CX, Sieling F, Pan H, Cui J. (2004). Ultrasound-induced cell membrane porosity. *Ultrasound Med Biol* 30:519–26.
- Dokukin ME, Sokolov I. (2012). Quantitative mapping of the elastic modulus of soft materials with HarmoniX and PeakForce QNM AFM modes. *Langmuir* 28:16060–71.
- Gelderblom E, Wolbers F, De Jong N, et al. (2013). Time-resolved high-speed fluorescence imaging of bubble-induced sonoporation. *POMA* 19:1–6.
- Grimaldi P, Di Giambattista L, Giordani S, et al. (2011). Ultrasound-mediated structural changes in cells revealed by FTIR spectroscopy: A contribution to the optimization of gene and drug delivery. *Spectrochim Acta A Mol Biomol Spectrosc* 84:74–85.
- Guzmán HR, Nguyen DX, Khan S, Prausnitz MR. (2001a). Ultrasound-mediated disruption of cell membranes. II. Heterogeneous effects on cells. *J Acoust Soc Am* 110:597–606.
- Guzmán HR, Nguyen DX, Khan S, Prausnitz MR. (2001b). Ultrasound-mediated disruption of cell membranes. I. Quantification of molecular uptake and cell viability. *J Acoust Soc Am* 110:588–96.
- Guzmán HR, Nguyen DX, McNamara AJ, Prausnitz MR. (2002). Equilibrium loading cells with macromolecules by ultrasound: effect of molecular size and acoustic energy. *J Pharm Sci* 91:1693–701.
- Karshafian R, Bevan PD, Williams R, et al. (2009). Sonoporation by ultrasound-activated microbubble contrast agents: effect of acoustic exposure parameters on cell membrane permeability and cell viability. *Ultrasound Med Biol* 35:847–60.
- Kodama T, Hamblin MR, Doukas AG. (2000). Cytoplasmic molecular delivery with shock waves: importance of impulse. *Biophys J* 79:1821–32.
- Krasovitski B, Frenkel V, Shoham S, Kimmel E. (2011). Intramembrane cavitation as a unifying mechanism for ultrasound-induced bioeffects. *Proc Natl Acad Sci U S A* 108:3258–64.
- Kuznetsova TG, Starodubtseva MN, Yegorenkov NI, et al. (2007). Atomic force microscopy probing of cell elasticity. *Micron* 38:824–33.
- Lee M-T, Hung W-C, Chen F-Y, Huang HW. (2008). Mechanism and kinetics of pore formation in membranes by water-soluble amphipathic peptides. *Proc Natl Acad Sci U S A* 105:5089–92.
- Lionetti V, Fittipaldi A, Agostini S, et al. (2009). Enhanced caveolae-mediated endocytosis by diagnostic ultrasound *in vitro*. *Ultrasound Med Biol* 35:136–143.
- Mason TJ. (2011). Therapeutic ultrasound an overview. *Ultrason Sonochem* 18:847–52.
- Meijering BDM, Juffermans LJM, van Wamel A, et al. (2009). Ultrasound and microbubble-targeted delivery of macromolecules is regulated by induction of endocytosis and pore formation. *Circ Res* 104:679–87.
- Mitragotri S. (2005). Healing sound: the use of ultrasound in drug delivery and other therapeutic applications. *Nat Rev Drug Discov* 4:255–60.
- Mourant JR, Gibson RR, Johnson TM, et al. (2003). Methods for measuring the infrared spectra of biological cells. *Phys Med Biol* 48:243–57.
- Newman CMH, Bettinger T. (2007). Gene therapy progress and prospects: ultrasound for gene transfer. *Gene Ther* 14:465–75.
- O'Brien WD. (2007). Ultrasound-biophysics mechanisms. *Prog Biophys Mol Biol* 93:212–55.
- Parasassi T, Gratton E, Yu WM, et al. (1997). Two-photon fluorescence microscopy of laurdan generalized polarization domains in model and natural membranes. *Biophys J* 72:2413–29.
- Schlicher RK, Radhakrishna H, Tolentino TP, et al. (2006). Mechanism of intracellular delivery by acoustic cavitation. *Ultrasound Med Biol* 32:915–24.
- Sundaram J, Mellein BR, Mitragotri S. (2003). An experimental and theoretical analysis of ultrasound-induced permeabilization of cell membranes. *Biophys J* 84:3087–101.
- Ward M, Wu J, Chiu JF. (2000). Experimental study of the effects of Optison concentration on sonoporation *in vitro*. *Ultrasound Med Biol* 26:1169–75.

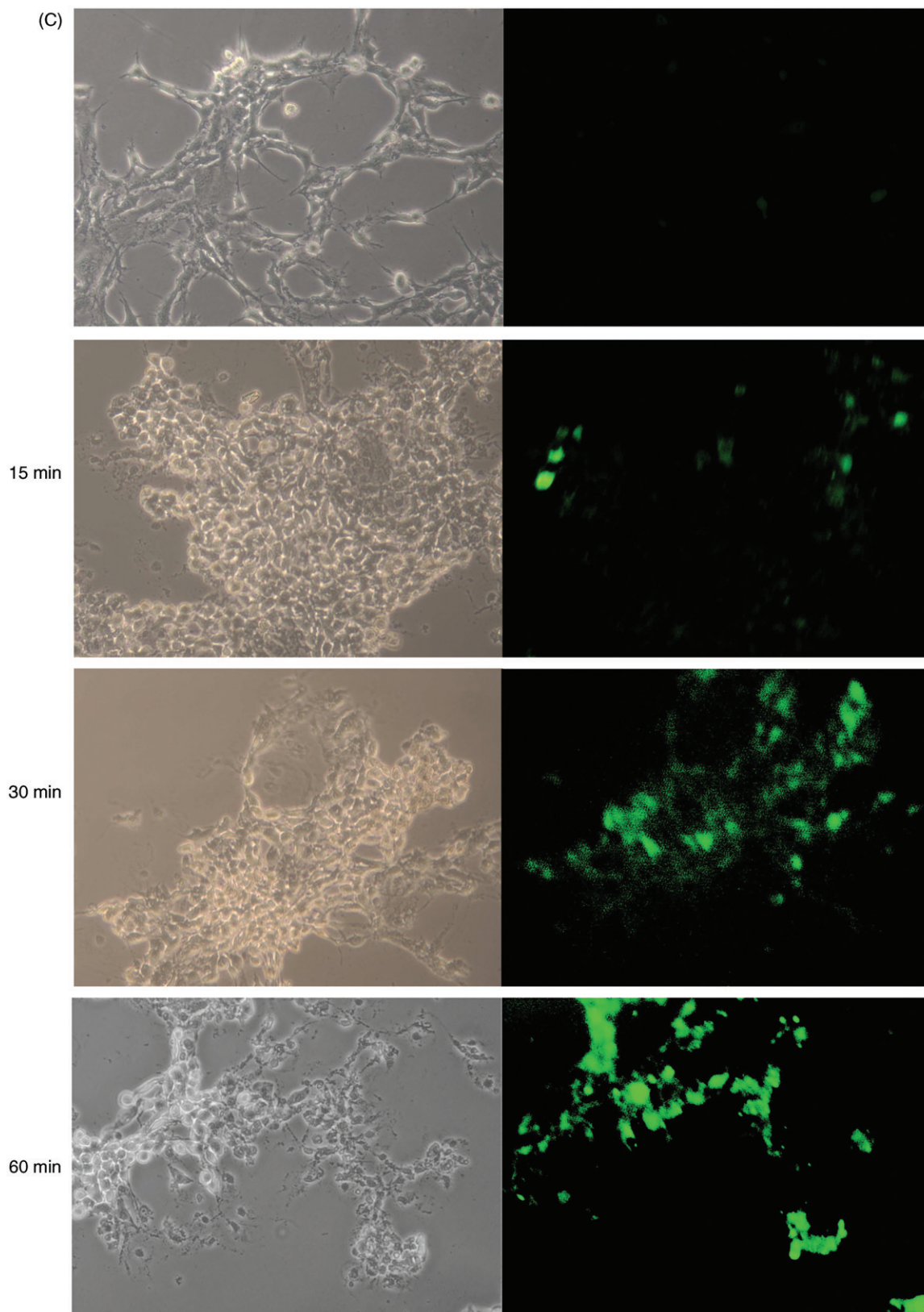


### Appendix: Photographic documentation of optical measurements

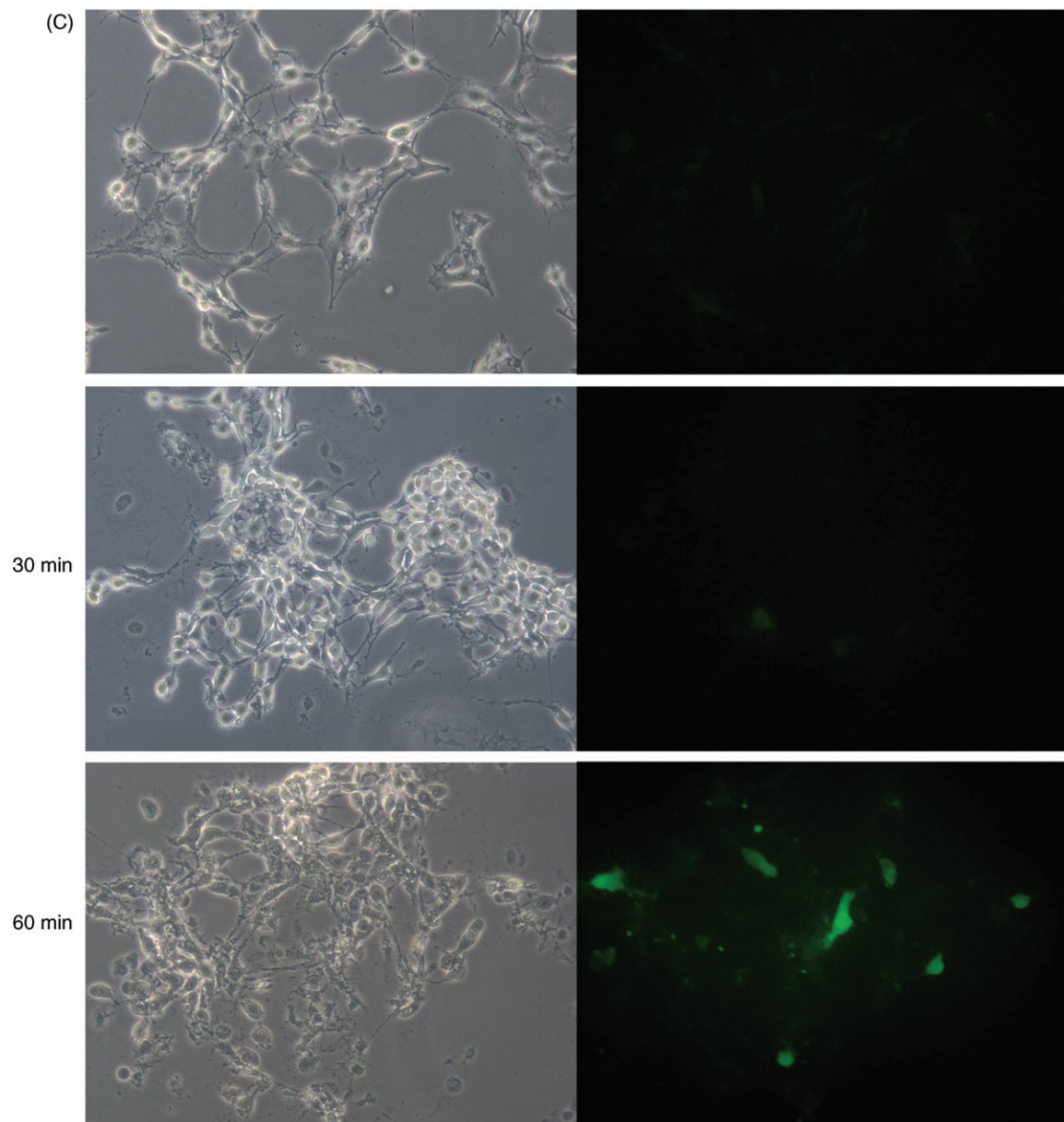
Representative set of images of murine fibroblasts NIH-3T3 cells obtained using a 10× objective (100× total magnification) of the inverted, phase contrast fluorescence microscope Leica DMIL, endowed with a 100 W mercury vapour lamp, FITC filter set, and coupled with high resolution and sensitivity CCD photocams (Jenoptik and Zeiss AxioCam ICc3) driven by Zen 2011 software. Cells were exposed to ultrasound at fixed  $I_{ta}$  11.8 mW/cm<sup>2</sup> for three times (15, 30 and 60 min) in presence of 10 μM of FITC labeled Dextrans at MW of 10 kDa, 40 kDa and 70 kDa.



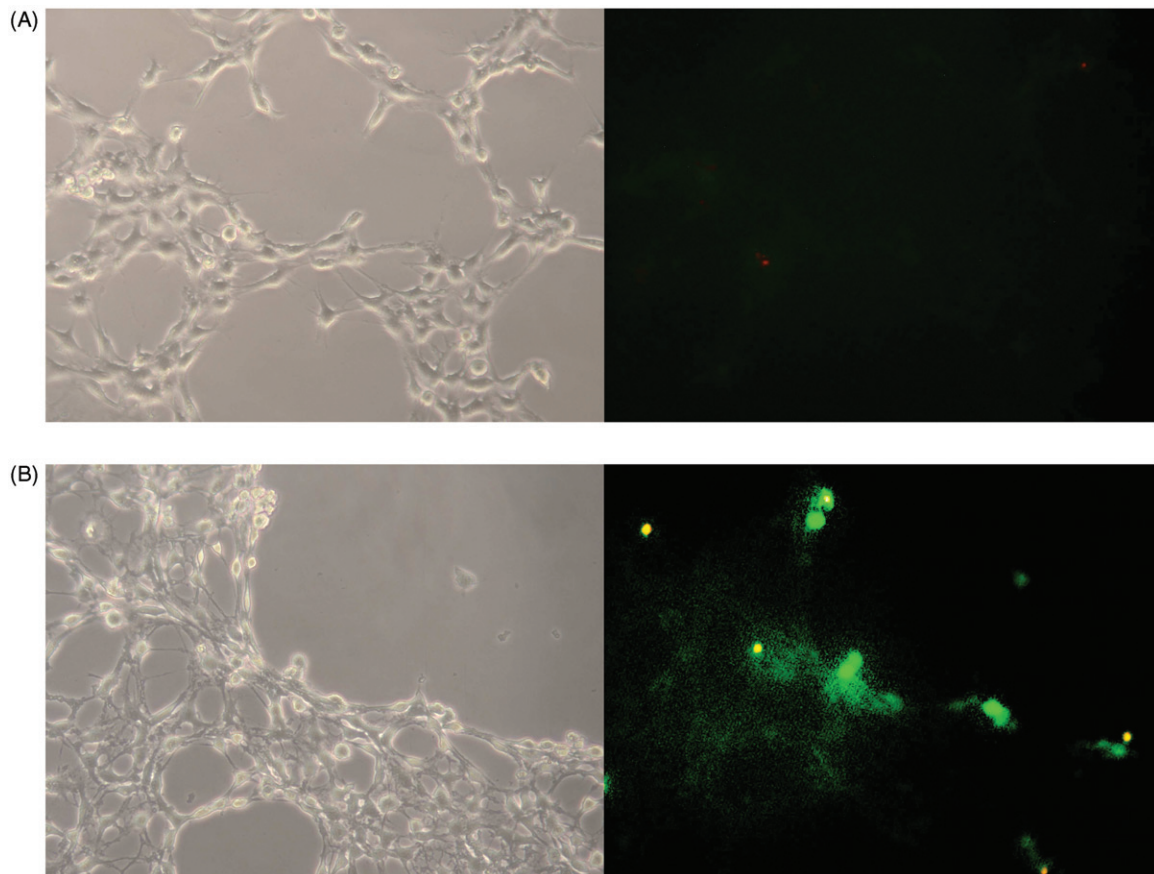
Dextran 10 kDa: the control (C) is shown in the first row; transmitting and epiluminescence microscopy images are shown in left side and right side of the panel, respectively.



Dextran 40 kDa: the control (C) is shown in the first row; transmitting and epifluorescence microscopy images are shown in left side and right side of the panel, respectively.



Dextran 70 kDa: the control (C) is shown in the first row; transmitting and epiluminescence microscopy images are shown in left side and right side of the panel, respectively.



A: control cells incubated with Dextran 70 kDa at 60' and Propidium Iodide; B: cells treated with US ( $I_{ta}$  11.8 mW/cm<sup>2</sup>) and Dextran 70 kDa at 60' including Propidium Iodide test.